Cement & Concrete Composites 61 (2015) 44–52

Contents lists available at ScienceDirect

Cement & Concrete Composites

journal homepage: www.elsevier.com/locate/cemconcomp

The hydration and microstructure of ultra high-strength concrete with cement–silica fume–slag binder

Caijun Shi *, Dehui Wang, Linmei Wu, Zemei Wu

College of Civil Engineering, Hunan University, Changsha 410082, China

ARTICLE INFO

Article history:
Received 14 December 2014
Received in revised form 5 March 2015
Accepted 28 April 2015
Available online 16 May 2015

Keywords:
Ultra high-strength concrete
Hydration
Microstructure
Porosity
Calcium hydroxide content
Synergistic effect

ABSTRACT

This study investigated the flowability, compressive strength, heat of hydration, porosity and calcium hydroxide content of ultra-high-strength concrete (UHSC) with cement–silica fume–slag binder at 20 °C. The composition of the binder was designed using seven-batch factorial design method. The relationships between the binder composition and the properties were expressed in contours. Results showed that proper silica fume content could improve the flowability and compressive strength of UHSC, reduce the porosity and calcium hydroxide content of UHSC. Slag reduced the flowability, compressive strength, porosity, and calcium hydroxide content of UHSC to certain extent. The silica fume and slag demonstrated positive synergistic effects on the flowability and 3 d compressive strength, but have negative synergistic effects on the total heat of hydration, hydration heat when the time is infinitely long(P_0), 56 d compressive strength, porosity and calcium hydroxide content of UHSC.

1. Introduction

Cementitious materials with a compressive strength of over 150 MPa and exceptional durability properties attracted significant interest around the world since early 1990s. First defined as reactive powder concrete, it is now more generally described as ultra-high-performance concrete/ultra-high-strength concrete (UHPC/UHSC) [1]. UHSC is composed of cement and very fine powders such as crushed quartz, silica fume. UHSC exhibites as very dense microstructure and super ductility, especially after high temperature curing. Incorporation of steel fibers can greatly enhance the toughness of UHSC [2–4]. UHSC was firstly used in the Sherbrooke Pedestrian Bikeway Bridge Quebec, Canada, and its applications have gradually increased since then [5].

The phase content in UHSC does not change obviously after 7 days of hydration. The crystalline phase content in the ordinary concrete was considerably higher than that in UHPC [6]. The average C–S–H chain length is short, and the pozzolanic activity is weak at 20 °C. At 90 °C, heat curing does not only increase the pozzolanic activity of both silica fume and crushed quartz, but also increase the average C–S–H chain length. At 250 °C xonotlite formed [7,8]. UHSC has a very low porosity, which never exceeds 9% in volume in the pore diameter range of 3.75 nm to 100 μm. What's more, it is nil in the range of 3.75 nm to 100 μm for UHSC when it was cured between 150–200 °C [9].

In former studies, the binders of UHSC were often composed of cement and silica fume. Their studies were mainly focused on the hydration and microstructure of UHSC after heat curing. In recent years, many researchers started to use other mineral admixtures to substitute cement and silica fume. Fly ash and ground granulated blast furnace slag can be the substitutes for cement and silica fume. Researches on mechanical characteristic of UHSC with high content of mineral admixtures show satisfactory results [10]. Compared with ordinary UHSC, though the contents of cement and silica fume were prominently reduced, compressive strength of samples containing high content of mineral admixtures were still over 200 MPa with standard curing, 234 MPa with steam curing and 250 MPa with autoclave curing [11]. Limestone powder can be another substitute for silica fume. When the limestone powder, silica fume and ground granulated blast furnace slag content were 20%, 10% and 20%, the 28 d and after strengths of samples were higher than that without limestone powder [12]. Rice husk ash could be considered as a supplementary cementitious material at low content. There was a synergic effect between rice husk ash and silica fume on the compressive strength of UHSC, demonstrated by the fact that the sample made by the blend of 10% rice husk ash and 10% silica fume showed higher compressive strength than that of the control sample without rice husk ash or samples using other blends with silica fume [13].

* Corresponding author. Tel.: +86 731 88823937.
E-mail address: cshi@hnu.edu.cn (C. Shi).

http://dx.doi.org/10.1016/j.cemconcomp.2015.04.013
0958-9465/

It can be observed that other supplementary cementitious materials can also be used for prepare for UHSC. However, UHSC were prepared with cement and silica fume and the studies on hydration and microstructure of UHSC mainly focused on heat curing so far. If the UHSC were prepared with other supplementary cementitious materials, such as slag, fly ash, limestone powder and rice husk ash, the hydration and microstructure may demonstrate significant differences. Moreover, if the UHSC was cured under standard condition, not heat curing, the hydration and microstructure of UHSC may be also very different. However, the study on hydration and microstructure of UHSC with common supplementary cementitious materials under standard curing condition was very limited. Thus, this study investigated flowability, compressive strength, hydration and microstructure of UHSC with cement–silica fume–slag binder cured in water at 20 °C.

2. Raw materials and experimental and methods

2.1. Raw materials

Raw materials used in this study include Portland cement (PC), silica fume, slag, natural quartz sand, superplasticizer and water. PC was complied with the Chinese Standards GB175-2007 and had Blaine fineness of 353 m^2/kg and particle size distribution as shown Fig. 1(a). Its chemical composition is given in Table 1. Silica fume (SF) is very fine with particle size approximately 0.1–0.2 μm, which exists in grey powder form and contains reactive silicon dioxide and no chloride or other potentially corrosive substances. The chemical composition of the silica fume is given in Table 1. The chemical composition of slag (S) is presented in Table 1. Its particle size distribution is given in Fig. 1(b).

Natural quartz sand was used as aggregate with maximum particle size of 2.36 mm. Polycarboxylate based superplasticizer (SP) was used.

2.2. Mixture proportions, specimen preparation and curing

The mixing proportion of UHSC was: binder materials: sand: water: superplasticizer = 1:1:0.16:0.02 by mass. The binder composition of UHSC was designed using factorial design method, as shown in Table 2 and Fig. 2. Initially dry materials (cement, silica fume, slag and natural quartz sand) were mixed using a high speed mixer for 1 min. Water and superplasticizer were added and mixed for about 3 min at a low speed, and then mixed for about 8 min at a high speed until the mixtures were uniform. When UHPC mixture was ready, it was casted into 40 × 40 × 160 mm and Φ10 × 150 mm cylinder moulds by two layers, and were vibrated 60 times at each layer to consolidate the mixtures. The specimens with moulds were kept in a room at about 20 °C for 24 h. The cast moulds were covered by plastic sheets until demoulding to prevent moisture losing. After demoulding, specimens were cured in calcium hydroxide saturated solution at 20 °C until testing ages.

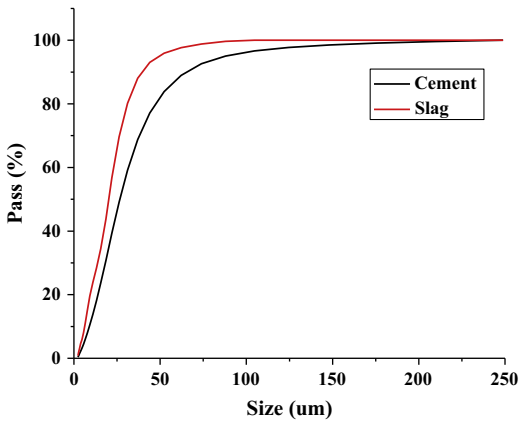

Fig. 1. Particle size distribution of PC and slag.

2.3. Experimental methods

2.3.1. Heat of hydration

The hydration heat was determined using an isothermal calorimeter. Binder components were put into a compulsory paste mixer at a high speed mixer for 1 min. Water and superplasticizer were added to the mixer at W/B of 0.16 and mixed for about 3 min with a low speed, and then mixed for about 8 min at a high speed. About 4 g paste samples was weighed and filled into a glass bottle then placed into TAM Air isothermal calorimeter immediately for measurement of heat of hydration. When the glass bottle were place into TAM Air isothermal calorimeter, the data acquisition system was initiated at the same time to record the output voltage from which the heat flow in the system could be calculated. All measurements were lasted for 72 h.

2.3.2. Flowability

The flowability of all mixtures was measured in accordance with the Chinese Standards GB/T 2419-2005. The mixtures were cast into mould by two layers. The first layer was casted to 2/3 height of mould, and the mixture was librated 15 times by a tamper. Then, the second layer was casted and librated. The mould was lifted lightly. The mixture was librated 25 times at flop table. The diameter of mixture was recorded.

2.3.3. Compressive strength

The strengths were measured using 40 × 40 × 160 mm specimens. The compressive strength was measured following Chinese Standards GB/T 17671-1999. The flexural strengths were conducted on three specimens from the same mixture, and compressive strengths were conducted on the six broken halves. The test results were averaged for the flexural strength and compressive strength.

2.3.4. Water absorption porosity

Specimens with the size of Φ10 × 150 mm cylinder were cast for porosity testing. The samples were cut from Φ10 × 150 mm cylinder, and sliced into Φ10 × 5 mm thin discs, then cured in calcium hydroxide saturated solution at 20 °C until testing ages. The total porosity of specimens was measured as follows: once the thin discs had been saturated under vacuum for 24 h, put the discs on a wire netting; the specimens were immersed in a bucket containing water and were linked to the weighing scale with a fishing line; then the weight of specimens saturated in the water was determined corresponds to w_2; determining the saturated surface dry basis weights corresponds to w_3; determining of the weight after drying up to constant mass at 105 °C corresponds to w_1; total water porosity = $(w_3 - w_1) \times 100/(w_3 - w_2)$.

2.3.5. Calcium hydroxide

The calcium hydroxide (CH) content in cement paste was measured quantitatively by thermogravimetric analysis. Samples were broken into pieces by a hammer. These samples were immersed in the absolute alcohol solution for 1 d to terminate hydration. Then, these samples were ground to powder until all the powders were passed through 0.045 mm sieve. After that, these powder were put into a vacuum oven at 60 °C for 24 h. The samples were selected randomly about 10 g to measure the calcium hydroxide content. The experiment temperature was ranging from room temperature to 1000 °C in a nitrogen environment at a constant

Table 1
Chemical composition of PC, silica fume and slag.

Chemical composition	SiO_2	Al_2O_3	Fe_2O_3	CaO	MgO	SO_3	Na_2O_{eq}	f-CaO	Loss	CL^-
PC	25.26	6.38	4.05	64.67	2.68	2.66	0.56	0.82	2.59	0.007
Silica fume	90.82	1.03	1.50	0.45	0.83					
Slag	33	13.91	0.82	39.11	10.04					

Table 2
Binder compositions of UHSC.

No	PC (%)	SF (%)	S (%)
N1	100	0	0
N2	85	15	0
N3	75	0	25
N4	72.2	11.1	16.7
N5	70	30	0
N6	58.3	16.7	25
N7	50	0	50

heating rate of 10 °C/min. The proportion of $Ca(OH)_2$ content to residual mass was then calculated.

2.4. Drawing contours in triangle coordinate system

The relation among x, y and z in triangular coordinate system should satisfy $x + y + z = 100\%$. Therefore, a corresponding relation between triangular coordinate systems and rectangular coordinate system could be established, as shown in Fig. 3 and formula (1). According to experimental results, contours can be drawn by some analysis software.

$$\begin{cases} x' = (x - 0.5) + \frac{\sqrt{3}}{2}y \\ y' = \frac{\sqrt{3}}{2}y \end{cases} \quad (1)$$

where
x', y' refer to the rectangular coordinate system,
x, y refer to the triangular coordinate system.

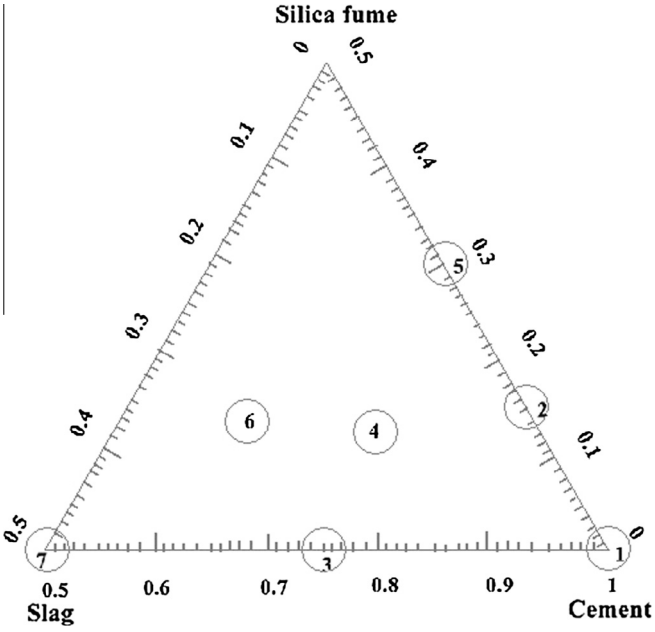

Fig. 2. Composition design in cement–silica fume–slag ternary cementitious system (mass ratio).

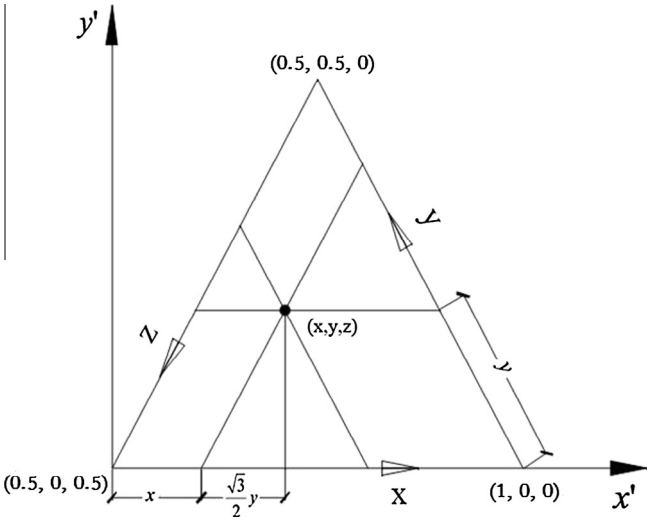

Fig. 3. Relation between triangular coordinate system and rectangular coordinate system.

2.5. Factorial design of ternary cementitious materials

The seven-batch factorial design method used in this study is commonly called simplex-centroid design [14]. If the mixture is composed of three components x_1, x_2 and x_3, then:

$$Y = \beta_1 x_1 + \beta_2 x_2 + \beta_3 x_3 + \beta_{12} x_1 x_2 + \beta_{23} x_2 x_3 + \beta_{13} x_1 x_3 + \beta_{123} x_1 x_2 x_3 \quad (2)$$

where
Y = responses, including any structural and property characteristics of ternary cementitious materials,
β_i is the coefficient,
x_1, x_2 and x_3 are the portions of the three components.

This method has been successfully used to study how the ternary cementitious composition affected strength or to predict the strength of ternary cementitious materials [15,16] and alkali–aggregate reaction expansion [17]. In this study, the seven-batch factorial design was used for the composition of binders. Then, equations were obtained to correlate the composition of cement–silica fume–slag ternary binders and the properties of UHSC. The response contour plots for the ternary cementitious system can be obtained in a ternary diagram using commercial software Surfer.

3. Results and discussion

The flowability, compressive strength, porosity and $Ca(OH)_2$ contents of UHSC are summarized in Table 3. The results are plotted and discussed in detail in the following sections.

3.1. Flowability

The flowabilities of UHSC with cement–silica fume–slag binders are shown in Fig. 4. From Fig. 4, it can be seen that in general, the

Table 3
Flowability, compressive strength, porosity and $Ca(OH)_2$ contents of UHSC.

No	Flowability (mm)	Compressive strength (MPa)		Porosity (%)		$Ca(OH)_2$ content (%)	
		3 d	56 d	3 d	56 d	3 d	56 d
N1	163	79.0	108.8	14.70	9.13	7.50	14.71
N2	156	82.8	123.3	12.82	8.82	6.64	4.64
N3	106	77.3	113.7	13.56	9.56	6.65	5.65
N4	146	80.1	126.9	12.97	8.97	6.57	4.57
N5	151	83.8	115.6	12.71	8.21	6.39	3.29
N6	198	84.0	116.9	12.65	8.75	6.28	4.28
N7	102	74.5	106.2	14.10	10.60	6.43	5.13

flowability of UHSC increased from 110 mm to 195 mm as the silica fume content increased from 0% to 22%, especially when slag content was more than 10%. However, when silica fume content was higher than 22%, the flowability of the mixtures was decrease. Since the particle size of silica fume is very fine, it would absorb much superplasticizer on the surface [18]. On the other hand, high water demand of silica fume could be counteracted by using superplasticizer instead of using relatively large amount of additional water [19]. Combined with superplasticizer, the silica fume contributes to the dispersion action of flocculated cement particles as ultra-fine particles, which could release more free water [20]. For ordinary concrete, the silica fume content is usually less than 10%. For the production of high strength and durable concrete, a combination of 10% silica fume with superplasticizer was necessary to maintain specified slump [21]. The silica fume content was usually less than 15% for high-performance concrete [22]. As for UHSC mixtures in this study, if silica fume content was low, it would not show evident dispersion action; if silica fume content was more than 22%, it would cause very cohesive and low flowable UHSC mixtures. Therefore, the proper dosage of silica fume for UHSC was larger than that for ordinary concrete or HPC.

The slag also evidently affected the flowability of the mixtures because its specific surface area was larger than that of the cement and required more water to achieve the same flowability. When the slag replacement was beyond 40%, the flowability of UHSC was less than 140 mm.

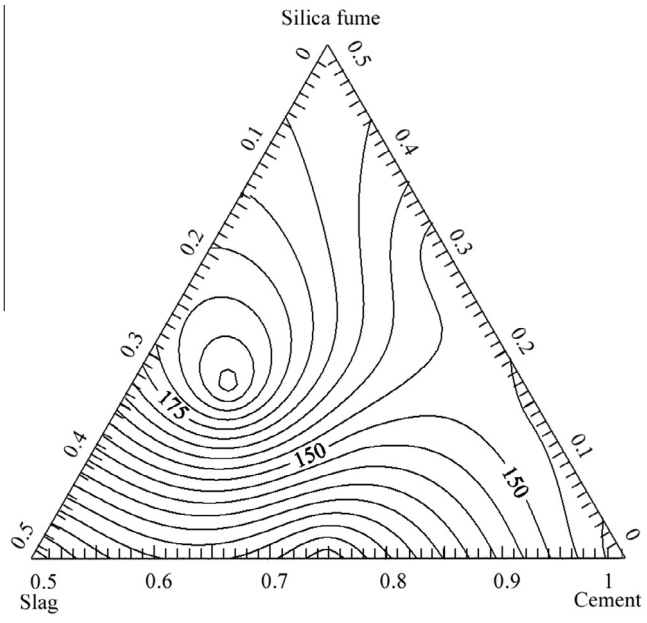

Fig. 4. Flowability contours of UHSC with cement–silica fume–slag binder.

Based on the flowability of the seven batches of UHSC, Eq. (2) could be solved, then the relationship between the flowability Y and the ternary binder composition can be described by Eq. (3):

$$Y = 1.63x_1 + 1.54x_2 + 2.53x_3 - 0.0044x_1x_2 + 0.46x_2x_3 - 0.042x_1x_3 - 0.0046x_1x_2x_3 \quad (3)$$

From Eq. (3), it can be seen that β_1, β_2, β_3 are positive, which indicates that the cement, silica fume and slag contents were conduced to the flowability of UHSC, and the effect of slag on flowability of UHSC was much obvious than that of cement and silica fume. β_{23} is positive, which indicates that the combination of silica fume and slag had positive synergistic effects on the flowability of UHSC.

3.2. Heat of hydration

Fig. 5(a) shows the heat evolution rate of UHSC. The rate of heat of hydration of the mixture with 15% silica fume (N2) surpassed that with Portland cement (N1) as shown in Fig. 5(a). When the silica fume content increased from 0% to 15%, the accelerated hydration decreased from 7.23 h to 4.77 h. However, when the silica fume content increased to 30% (N5), the rate of heat of hydration slowed and the accelerated hydration increased to 6.37 h. The results indicate that the addition of 30% silica fume altered the hydration process after the start of hydration. The rate of acceleration period was reduced [23].

The results in Fig. 5(a) indicate that the peak of the heat flow of mixture with slag (N3, N7) appeared later than that with pure

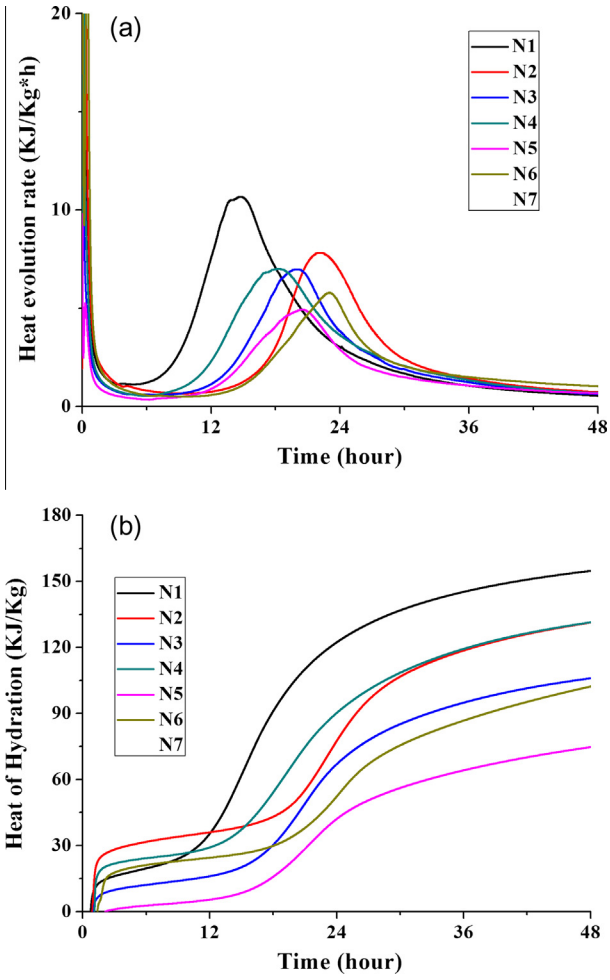

Fig. 5. Heat evolution of binder materials of UHSC.

Table 4
Values of P_0, t_0, t_{50}, and the equation.

No	P_0 (kJ/kg)	t_0 (h)	t_{50} (h)	Equation
N1	228	7.23	17.07	$P = 228 \times \frac{t-7.23}{(t-7.23)+17.07}$
N2	206	4.77	12.84	$P = 206 \times \frac{t-4.77}{(t-4.77)+12.84}$
N3	186	9.95	15.04	$P = 186 \times \frac{t-9.95}{(t-9.95)+15.04}$
N4	175	7.31	24.57	$P = 175 \times \frac{t-7.31}{(t-7.31)+24.57}$
N5	203	6.37	21.36	$P = 203 \times \frac{t-6.37}{(t-6.37)+21.36}$
N6	144	6.27	37.33	$P = 144 \times \frac{t-6.27}{(t-6.27)+37.33}$
N7	172	9.8	25.54	$P = 172 \times \frac{t-9.8}{(t-9.8)+25.54}$

Portland cement (N1). When the slag content was 25% and 50%, the accelerated hydration was 9.95 and 9.8 h, respectively. There was also a tendency for the curve of mixtures with silica fume and slag (N4, N6) to shift to the right, which indicated a slight retardation of hydration than that of mixture with silica fume only. Thus, slag retarded hydration mainly during the dormant and acceleration periods.

Fig. 5(b) shows the addition of 15% silica fume (N2) increased, but the addition of 30% silica fume (N5) decreased the total hydration heat of UHSC. Incorporation of slag (N3, N7) decreased the total hydration heat of UHSC.

Knudsen [24] suggested that the kinetics of cement hydration may be described by the following equation:

$$P = P_0 \cdot \frac{t - t_0}{(t - t_0) + t_{50}} \tag{4}$$

where

P = represented property (heat evolution, strength, chemical shrinkage etc.) at the time t,
t_0 = the time at the end of the induction period,
t_{50} = the time for 50% reaction degree,
P_0 = the property when the time is infinitely long.

In the present study, P represents heat evolution. If the experimental results of heat evolution of UHSC are plotted in reciprocal diagrams of $1/P$ verse $1/(t - t_0)$, several lines could be obtained, t_{50} and $1/P_0$ can be determined by extrapolating these lines. The values of P_0, t_0, t_{50}, and the equations are given in Table 4.

Based on the values of P_0, t_0, t_{50} in Table 4, then the relationship between P_0, t_0, t_{50} and the ternary binder composition can be obtained as follows:

$$Y_{p_0} = 2.2778x_1 + 4.4444x_2 + 2.2778x_3 - 0.0556x_1x_2 - 0.2222x_2x_3 - 0.0278x_1x_3 \tag{5}$$

$$Y_{t_0} = 0.072x_1 + 0.68x_2 + 0.0089x_3 - 0.009x_1x_2 - 0.025x_2x_3 + 0.0023x_1x_3 + 0.0003x_1x_2x_3 \tag{6}$$

$$Y_{t_{50}} = 0.17x_1 + 2.3x_2 + 0.84x_3 - 0.028x_1x_2 - 0.043x_2x_3 - 0.01x_1x_3 + 0.0012x_1x_2x_3 \tag{7}$$

From Eqs. (5)–(7), it can be seen that β_1, β_2, β_3 are positive, which indicates that the cement, silica fume and slag contents were conduced to the P_0, t_0, t_{50} of UHSC, and the effect of silica fume on P_0, t_0, t_{50} of UHSC was much evident than that of slag and cement. β_{23} is negative in all three equations, which indicated that the combination of silica fume and slag had negative synergistic effects on P_0, t_0, t_{50}.

From Fig. 6(a), it can be seen that P_0 increased with the increase of cement content or with the decrease of slag content. However,

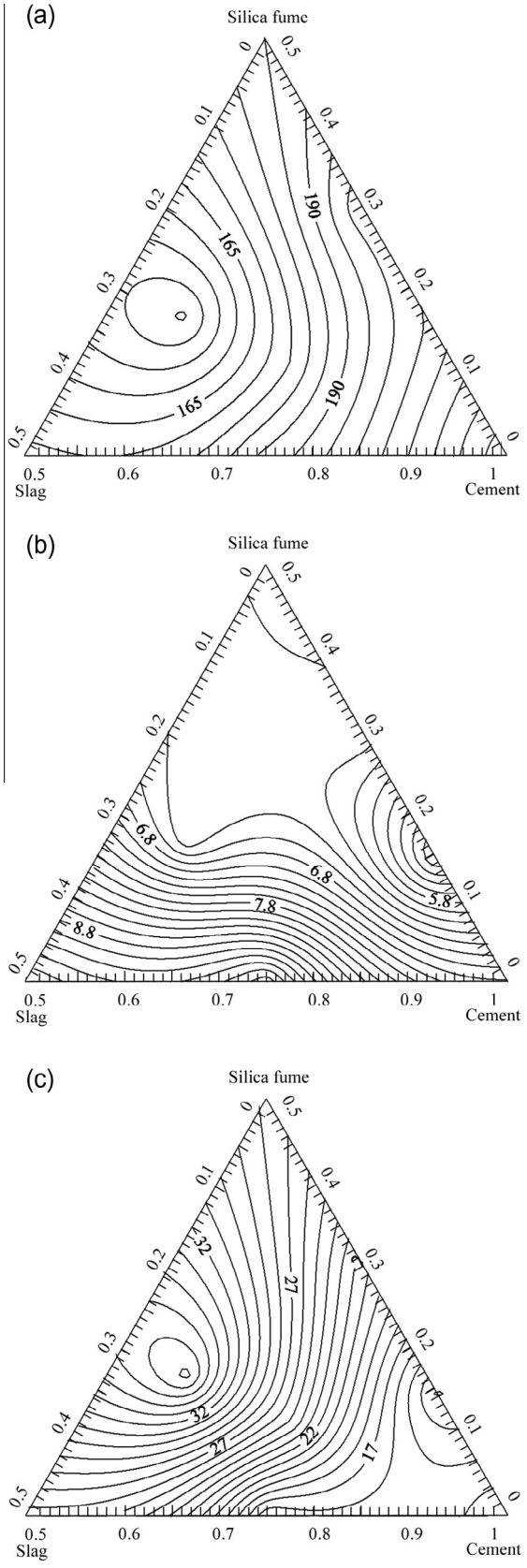

Fig. 6. Contours of different heat evolution parameters of UHSC mixtures with cement–silica fume–slag binder.

the effect of silica fume content on the P_0 was complicated, and there was an optimal content of silica fume for P_0 of UHSC.

From Fig. 6(b), it can be seen that t_0 decreased with the increase of silica fume content when the silica fume content was less than 20%, but the t_0 increased with the increase of slag content.

From Fig. 6(c), it can be seen that the t_{50} decreased with the increase of cement content, but the t_{50} increased with increase of slag content when its content did not exceed 30%. However, the effect of silica fume content on t_{50} was complicated. There was an optimal content of silica fume for t_{50} of UHSC.

3.3. Compressive strength

The compressive strengths of UHSC with cement–silica fume–slag binders are shown in Fig. 7. From Fig. 7(a), it can be seen that, at 3 days, the compressive strength of UHSC increased with the increase of silica fume content. However, when the silica fume content exceeded 25%, this trend was slacked. Silica fume had a positive effect on the early compressive strength of the mixtures due to its high pozzolanic activity and small particles. Amorphous SiO_2 in silica fume reacted with calcium hydroxide from the hydration of cement to form calcium–silicate–hydrate (C–S–H), which increased strength of UHSC at early age [25,26]. From Fig. 7(b), it can be seen that, the 56 d compressive strength of UHSC increased with the increase of silica fume content when it was less than 15%. When the silica fume content increased from 0% to 15%, the 56 d compressive strength of UHSC increased from 108 MPa to 125 MPa. Thus, concrete containing 10–15% slag and 15% silica fume could be considered as an optimum mixture for UHSC.

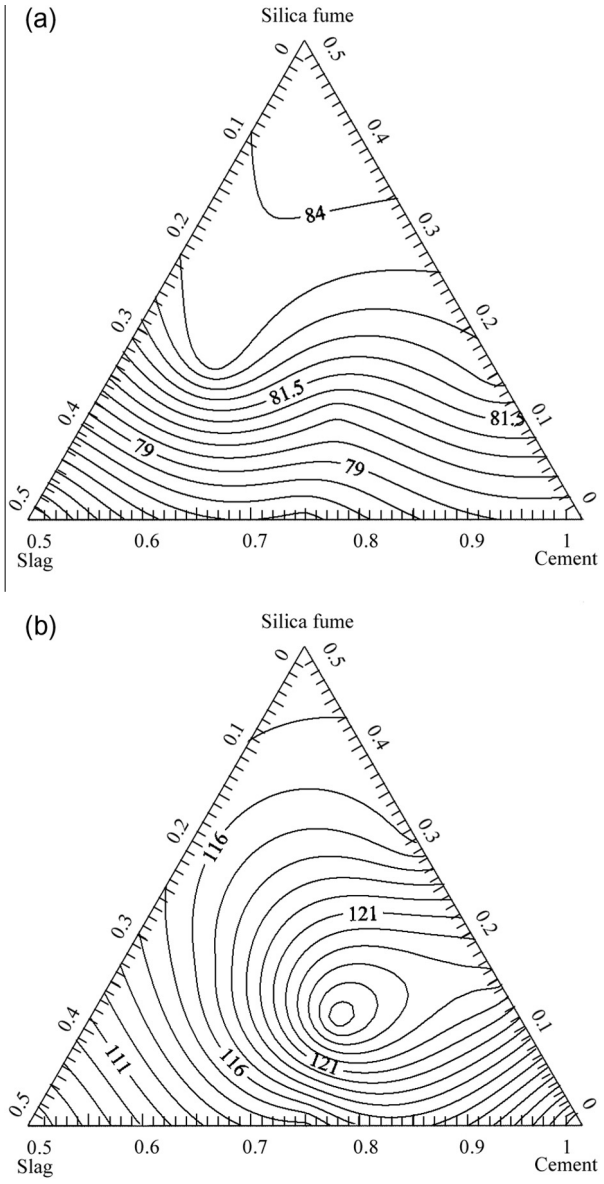

Fig. 7. Compressive strength of UHSC with cement–silica fume–slag binder at 3 and 56 days.

At 3 days, slag reduced the compressive strength of UHSC, especially, when the slag content exceeded 25%, the early compressive strength of UHSC deceased from 84 MPa to 78 MPa. At 56 days, when the slag content increased from 10% to 20%, the UHSC mixtures achieved the highest compressive strength of 125 MPa. It seemed that slag alone would decrease the compressive strength of UHSC. However, in combination with silica fume, slag could increase the compressive strength of UHSC. This was likely due to the appropriate combination of cementitious materials used, which yielded an approximate C/S ratio. It has been reported that the optimum combination of cementitious materials for high strength depended on the fineness of the siliceous materials and the C/S ratio [27,28]. Mixtures having CaO/SiO_2 ratio of 1.30 performed generally better than mixtures with constant and high amount of silica fume [11]. The C/S ratio of UHSC mixtures in this study were 2.36, 1.42, 2.02, 1.46, 0.91, 1.17 and 1.74, respectively. Theoretically, silica fume could remarkably reduce the C/S ratio, thus it could increase the compressive strength of UHSC with increased silica fume content. Incorporation of slag is another method to reduce the C/S ratio of the mixtures. However, slag reduced the flowability of mixtures so that it would increase the porosity of UHSC mixtures. Therefore, combined with silica fume, slag content could improve compressive strength of UHSC mixtures. In previous studies, compressive strength of UHSC containing fly ash and ground blast furnace reached 281 Mpa [11], which was much larger than that of UHSC mixtures in this study. It is because the specimens contained 3% brass coated steel fibers (by volume) and were autoclaved at 210 °C under 2.0 MPa pressure for 8 h.

Based on the compressive strength of the seven mixtures of UHSCs, Eq. (2) could be solved, and the relationship between the compressive strength Y and the ternary binder composition can be established by Eqs. (8) and (9):

$$Y_3 = 0.79x_1 + 0.51x_2 + 0.66x_3 + 0.0062x_1x_2 + 0.062x_2x_3 + 0.0009x_1x_3 - 0.0008x_1x_2x_3 \quad (8)$$

$$Y_{56} = 1.09x_1 - 2.14x_2 + 0.54x_3 + 0.049x_1x_2 - 0.098x_2x_3 + 0.0099x_1x_3 + 0.0022x_1x_2x_3 \quad (9)$$

From Eq. (8), it can be seen that β_1, β_2, β_3 are positive at 3 day, which indicates that the cement, silica fume and slag content were conduced to the compressive strength of UHSC at early age. From Eq. (9), it can be seen that β_1, β_3 are positive, but β_2 is negative at 56 day, which indicates that cement and slag content increased the compressive strength, but silica fume decreased the compressive strength of UHSC at later age. The effect of cement on compressive strength of UHSC was much notable than that of slag and silica fume. From Eqs. (8) and (9), it can be seen that β_{23} is positive at 3 day and is negative at 56 day, which indicate that the silica fume and slag had positive synergistic effect on the 3 d compressive strength, but negative synergistic effect on the 56 d compressive strength of UHSC.

3.4. Porosity in UHSC

The porosities of UHSC with cement–silica fume–slag binders are shown in Fig. 8. From Fig. 8(a), it can be seen that the porosity

of UHSC decreased with the increase of silica fume content. When the silica fume content increased from 0% to 50%, the 3 d porosity decreased from 14% to 12.7%, and the 56 d porosity decreased from 10.4% to 8.3%. At higher silica fume content, the capillary porosity was lower. It is generally accepted that the silica fume improves pore structure in two ways: its filler effect in which the silica fume particles bridge the spaces between cement grains and the spaces between cement grains and aggregate; and pozzolanic effect in which silica fume reacts with calcium hydroxide to produce more C–S–H gel leading to an additional reduction in pore size and capillary porosity during hydration [29,30].

It is observed that at 3 days, if the silica fume content was more than 25% and the slag content was less than 25%, slag had little effect on the porosity of UHSC. However, at 56 days, any slag content increased the porosity of UHSC. On one hand, slag could reduce the flowability of UHSC and improve the porosity of UHSC. On the other hand, at the early age, when UHSC samples were cured in calcium hydration saturated solution, slag was activated to consume $Ca(OH)_2$ and additional C–S–H formed and decreased the porosity of UHSC. However, at later age, the compressive strength of UHSC was sufficiently developed and the porosities of UHSC were relatively low. Thus, slag could not contact saturated calcium hydration solution and became latent activated that it could not participate to the hydration reaction to decrease the porosity of UHSC.

In this study, the porosities of UHSC mixtures ranged from 12.7% to 14% at 3 days, and from 8.3% to 10.4% at 56 days. However, it has been reported that the porosity of UHSC never exceeded 9% in volume in the pore diameter range of 3.75 nm to 100 μm in a previous study [9]. The UHSC mixtures of the previous study were pressed and heat cured, and their porosities were tested by Mercury Intrusion Porosimetry. However, in this study, the UHSC mixtures were cured at room temperature and their porosities were tested by water absorption. As for Mercury Intrusion Porosimetry, largest capillary pores, saturated at low pressures, are not measured. On the other side, porosity by water adsorption measured the total open porosity of materials [31].

Based on measured porosity of the seven batches of UHSCs, Eq. (2) could be solved, then the relationship between the porosity Y and the ternary binder composition can be described by Eq. (10), (11):

$$Y_3 = 0.15x_1 + 0.36x_2 + 0.2x_3 - 0.0039x_1x_2 - 0.0096x_2x_3 - 0.0013x_1x_3 + 0.0001x_1x_2x_3 \quad (10)$$

$$Y_{56} = 0.091x_1 + 0.014x_2 + 0.15x_3 + 0.0007x_1x_2 - 0.0013x_2x_3 - 0.0005x_1x_3 \quad (11)$$

From Eq. (10), (11), it can be seen that β_1, β_2, β_3 are positive, which indicates that the cement, silica fume and slag content were conduced to the porosity of UHSC. It can also inferred that the effect of silica fume on porosity of UHSC at early age was much obvious than that of slag and cement, and the effect of slag on porosity of UHSC at later age was much obvious than that of cement and silica fume. β_{23} is negative, which indicates that the combination of silica fume and slag had negative synergistic effect on the porosity of UHSC.

Based on experimental results above, relation between compressive strength and porosity of UHSC could be established, as shown in Fig. 9. The relation between compressive strength and porosity of UHSC was: $y = 245.92 \times e^{-0.0832x}$, and correlation coefficient was 0.92207.

3.5. Calcium hydroxide content

The calcium hydroxide contents of UHSC with cement–silica fume–slag binders are shown in Fig. 10. It can be seen that the

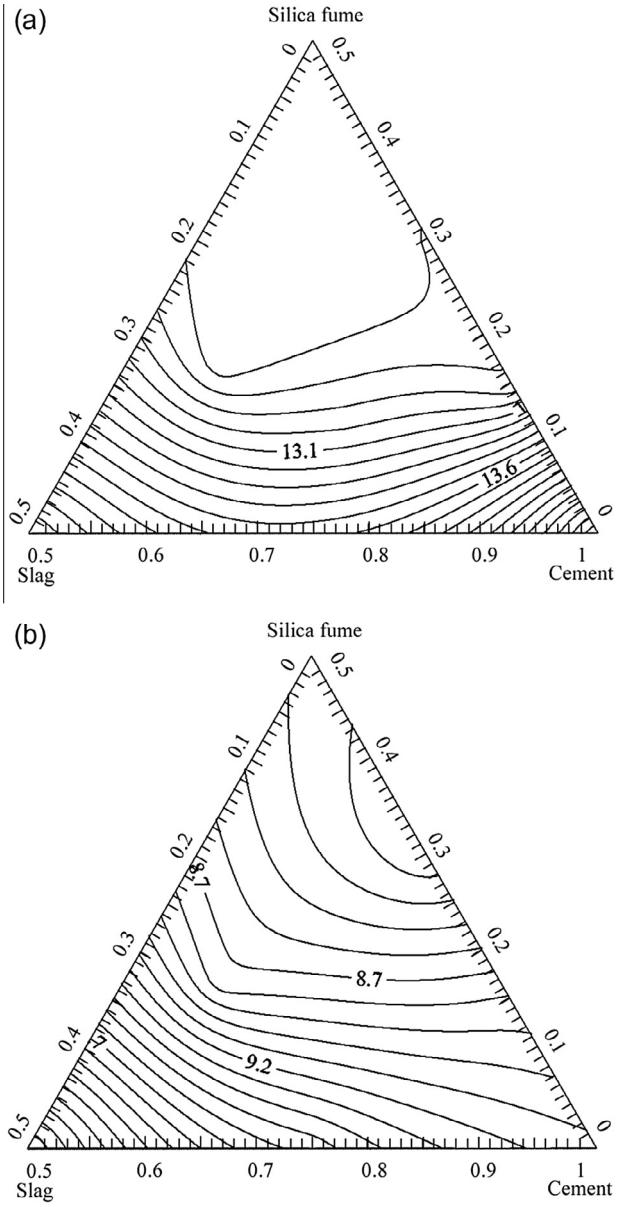

Fig. 8. Porosity of UHSC with cement–silica fume–slag binder at 3 and 56 days.

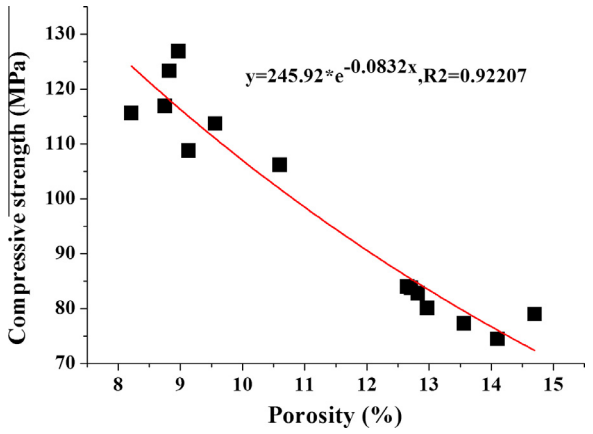

Fig. 9. Relationship between compressive strength and porosity of UHSC.

calcium hydroxide content decreased with increase silica fume content. When the silica fume content increased from 0% to 50%, the calcium hydroxide content decreased from 7.4% to 6.25%. However, the effect of slag on calcium hydroxide content was very limited. When silica fume was used to replace cement, it acts as a pozzolan to react with calcium hydroxide from the hydration of cement [32–34]. As shown in Table 1, silica fume contained 0.45% CaO, but slag contained 39.11% CaO, therefore, the effect of silica fume on the content of calcium hydroxide was distinct.

Typically, the initial calcium hydroxide contents depend mainly on the fraction of cement content in the matrix. Therefore, it was clearly seen that the mixtures with higher content of slag or silica fume showed less initial calcium hydroxide contents at 3 days. After that, the calcium hydroxide contents were further reduced due to the pozzolanic reaction. The calcium hydroxide contents decreased with the increasing of slag or silica fume content [35].

Based on measured calcium hydroxide content of seven batches of UHSCs, Eq. (2) could be solved, and the relationship between calcium hydroxide content and the ternary binder composition are shown in Eqs. (12) and (13):

$$Y_3 = 0.075x_1 + 0.13x_2 + 0.079x_3 - 0.0014x_1x_2 - 0.0041x_2x_3 - 0.0005x_1x_3 + 0.0001x_1x_2x_3 \quad (12)$$

$$Y_{56} = 0.15x_1 + 1.12x_2 + 0.3x_3 - 0.019x_1x_2 - 0.027x_2x_3 - 0.0068x_1x_3 + 0.0004x_1x_2x_3 \quad (13)$$

From Eqs. (12) and (13), it can be seen that β_1, β_2, β_3 are positive, which indicates that the content of cement, silica fume and slag were conduced to the calcium hydroxide content of UHSC, and the effect of silica fume on calcium hydroxide is much notable than that of slag and cement. β_{23} is negative, which indicates that the combination of silica fume and slag had negative synergistic effect on the calcium hydroxide content of UHSC.

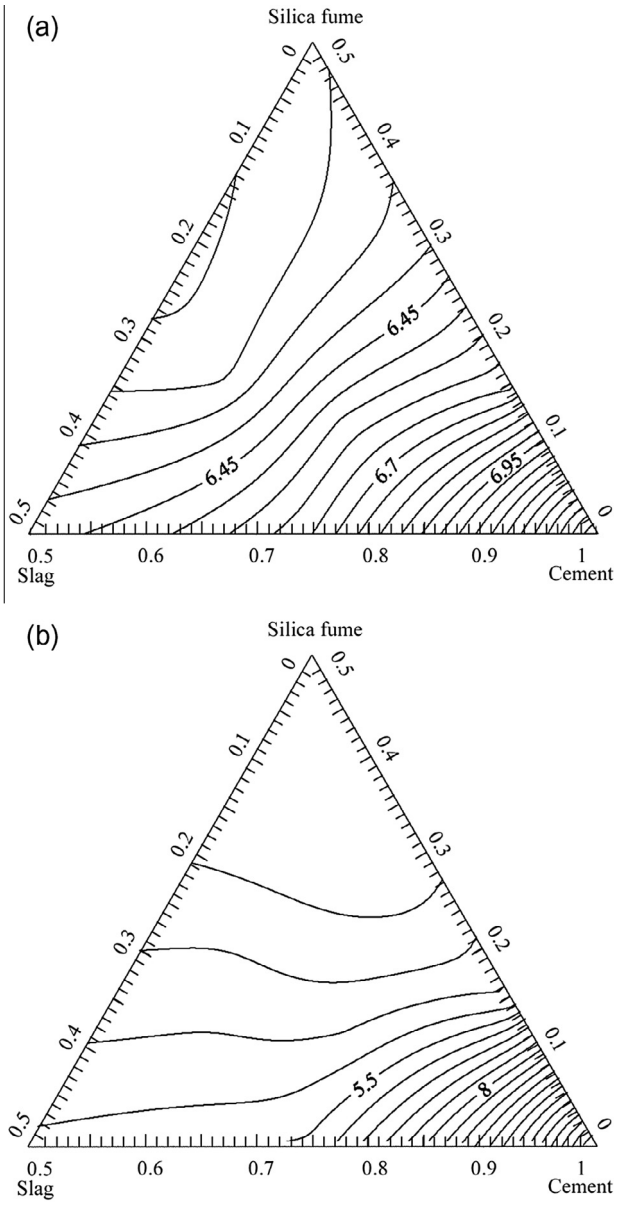

Fig. 10. Calcium hydroxide content of UHSC with cement–silica fume–slag binder at 3 and 56 days.

4. Conclusions

In this study, the hydration and microstructure of UHSC with cement–silica fume–slag binder were studied. The following conclusions can be drawn:

Silica fume could improve the flowability of UHSC, but the silica fume content should be in an appropriate range. When the silica fume content increased from 0% to 22%, the flowability of UHSC increased from 110 mm to 195 mm. However, when the silica fume content was more than 22%, the flowability of UHSC decreased. Slag would decrease the flowability of UHSC, the slag amount should not exceed 40% of the binder. When the slag content exceeded 40%, the flowability of UHSC was less than 140 mm. Combination of silica fume and slag demonstrated positive synergistic effect on the flowability of UHSC.

Silica fume altered the hydration after the induction period and reduced the rate of accelerated hydration. The rate of hydration heat of the mixture with 15% silica fume surpassed that with Portland cement. When the silica fume content increased from 0% to 15%, the accelerated hydration decreased from 7.23 h to 4.77 h. However, when the silica fume content increased to 30%, the rate of hydration heat of UHSC slowed and the accelerated hydration increased to 6.37 h. Slag retarded hydration mainly in the dormant and acceleration periods. When the slag content was 25% and 50%, the accelerated hydration was 9.95 and 9.8 h, respectively. The combination of silica fume and slag demonstrated negative synergistic effect on the P_0, t_0, t_{50}.

Silica fume increased the compressive strength of UHSC but the content should not exceed 25%. When the silica fume content increased from 0% to 15%, the 56 d compressive strength of UHSC increased from 108 MPa to 125 MPa. The slag reduced the early strength of UHSC. Especially, when the slag content surpassed 25%, the early compressive strength of UHSC deceased from 84 MPa to 78 MPa. In combination with silica fume, the highest compressive strength of 125 MPa could be achieved at later ages when slag content ranged from 10% to 20%. The silica fume and slag had positive synergistic effect on the 3 d compressive strength of UHSC, and negative synergistic effect on the 56 d compressive strength of UHSC.

The porosity of UHSC decreased with the increase of silica fume content due to the filling and pozzolanic effects of silica fume. When the silica fume content increased from 0% to 50%, the 3 d porosity decreased from 14% to 12.7%, and the 56 d porosity decreased from 10.4% to 8.3%. If the silica fume content was higher than 25% and slag content was less than 25%, slag had little effect on the porosity of UHSC at 3 days. However, slag at any content increased the porosity of UHSC at 56 days. The combination of

silica fume and slag had negative synergistic effect on the porosity of UHSC.

The calcium hydroxide content of UHSC decreased with the increase of silica fume content. When the silica fume content increased from 0% to 50%, the calcium hydroxide content decreased from 7.4% to 6.25%. However, the effect of slag content on the calcium hydroxide was limited. The combination of silica fume and slag had negative synergistic effect on the calcium hydroxide content of UHSC.

Acknowledgements

Financial supports from National Science Foundation of China under contract Nos. 51378196 and U1305243 are greatly appreciated.

References

[1] Kay W, Antoine EN, Gustavo JPM. Ultra-high performance concrete with compressive strength exceeding 150 MPa (22 ksi): a simpler way. ACI Mater J 2011:46–54 [January–February].
[2] Morin V, Cohen TF, Feylessoufi A, Richard P. Evolution of the capillary network in a reactive powder concrete during hydration process. Cem Concr Res 2002;32:1907–14.
[3] Chan Y, Chu S. Effect of silica fume on steel fiber bond characteristics in reactive powder concrete. Cem Concr Res 2004;34:1167–72.
[4] Shi CJ, Wu ZM, Wang DH, Wu LM. Design and properties of ultra high performance concrete. Johannesburg, South Africa: ICCMATS; 2014.
[5] Aitcin PC. Concrete the most widely used construction materials. ACI SP 1995;154:257–66.
[6] Korpa A, Kowald T, Trettin R. Phase development in normal and ultra high performance cementitious systems by quantitative X-ray analysis and thermoanalytical methods. Cem Concr Res 2009;39:69–76.
[7] Samuel P, Sylvie M, Hblbne Z, Pedro N, Vincent M, Marcel C. ^{29}Si NMR study of hydration and pozzolanic reactions in reactive powder concrete (RPC). Magn Reson Imaging 1996;14(7/8):891–3.
[8] Zanni H, Cheyrezy M, Maret V, Philippot S, Nieto P. Investigation of hydration and pozzolanic reaction in reactive powder concrete (RPC) using 29Si NMR. Cem Concr Res 1996;26(1):93–100.
[9] Cheyrezy M, Maret V, Frouin L. Microstructural analysis of RPC (reactive powder concrete). Cem Concr Res 1995;25(7):1491–500.
[10] Shi CJ, Xiao JF, Cao Z, Wang DH, Wu ZM, Ou ZH. Effects of UHPC constituents on its properties. Bull Chin Ceram Soc 2013;32(6):1005–11. 6.
[11] Yazici H. Utilization of fly ash and ground granulated blast furnace slag as an alternative silica source in reactive powder concrete. Fuel 2008;87:2401–7.
[12] Wang C. Preparation of ultra-high performance concrete with common technology and materials. Cement Concr Compos 2012;34:538–44.
[13] Nguyen VT. The study of using rice husk ash to produce ultra high performance concrete. Constr Build Mater 2011;25:2030–5.
[14] Wadsworth MH. Handbook of statistical methods for engineers and scientists. New York: McGraw-Hill; 1990.
[15] Wang D, Chen Z. On predicting compressive strengths of mortars with ternary blends of cement, GGBFS and fly ash. Cem Concr Res 1997;27:487–93.
[16] Shi C, Hu S. Cementitious properties of ladle slag fines under autoclave curing conditions. Cem Concr Res 2004;33(11):1851–6.
[17] Shi CJ, Shi ZG, Lu DY, He FQ. Research on alkali reactivity of sand and gravel from Xiangjiang River and conditions for safe Use. J Chin Ceram Soc 2011;39(1):13–9.
[18] Khatri RP, Sirivivatnanon V. Effect of different supplementary cementitious materials on mechanical properties of high performance concrete. Cem Concr Res 1995;25(1):209–20.
[19] Ganesh BK, Surya PPV. Efficiency of silica fume in concrete. Cem Concr Res 1995;25(6):1273–83.
[20] Duval R, Kadri EH. Influence of silica fume on the workability and the compressive strength of high-performance concretes. Cem Concr Res 1998;28(4):533–47.
[21] Khayat KH, Aitcin PC. Silica fume: a unique supplementary cementitious material. In: Ghosh SN, editor. Mineral admixtures in cement and concrete. ABI Books Private Limited; 1993. p. 227–65. vol. 4.
[22] Mazloom M, Ramezanianpour AA, Brooks JJ. Effect of silica fume on mechanical properties of high-strength concrete. Cement Concr Compos 2004;26(4):347–57.
[23] Rong ZD, Sun W, Xiao HJ, Wang W. Effect of silica fume and fly ash on hydration and microstructure evolution of cement based composites at low water–binder ratios. Constr Build Mater 2014;51:446–50.
[24] Knudsen T. 7th ICCC, vol. II, Parigi-Paris; 1980. p. I/170–5.
[25] Erdem TK, Kirca O. Use of binary and ternary blends in high strength concrete. Constr Build Mater 2008;22:1477–83.
[26] Elahi A, Basheer PAM, Nanukuttan SV, Khan QUZ. Mechanical and durability properties of high performance concretes containing supplementary cementitious materials. Constr Build Mater 2010;24:292–9.
[27] Taylor HFW. Cement chemistry. Thomas Telford Services Ltd.; 1997.
[28] Hong SY, Glasser FP. Phase relations in the CaO–SiO_2–H_2O system to 200 °C at saturated steam pressure. Cem Concr Res 2004;34(9):1529–34.
[29] Bentz DP, Stutzman PE. Evolution of porosity and calcium hydroxide in laboratory concretes containing silica fume. Cem Concr Res 1994;24:1044–50.
[30] Duan P, Shui ZH, Chen W, Shen CH. Effects of metakaolin, silica fume and slag on pore structure, interfacial transition zone and compressive strength of concrete. Constr Build Mater 2013;44:1–6.
[31] Ahmed HS, Said K, Luc C, Anne D. Microstructure and durability of mortars modified with medium active blast furnace slag. Constr Build Mater 2011;25:1018–25.
[32] Lu P, Sun G, Young JF. Phase composition of hydrated DSP cement pastes. J Am Ceram Soc 1993;76:1003–7.
[33] Zhang MH, Gjùrv OE. Effect of silica fume on cement hydration in low cement pastes. Cem Concr Res 1991;21:800–8.
[34] Ogawa K, Uchikawa H, Takemoto K, Yasui I. The mechanism of the hydration in the system C3S-pozzolana. Cem Concr Res 1980;10:683–96.
[35] Kritsada S, Lutz F. Evaluation of calcium hydroxide contents in pozzolanic cement pastes by a chemical extraction method. Constr Build Mater 2011;25:190–4.